European Journal of Wood and Wood Products
https://doi.org/10.1007/s00107-024-02085-z

ORIGINAL ARTICLE

Energy and structural optimization of mid-rise light-frame timber buildings for different climates and seismic zones in Chile

Alexander Wenzel[1,2] · **Sergio Vera**[2,3,4] · **Pablo Guindos**[1,2,5]

Received: 11 September 2023 / Accepted: 19 April 2024

Abstract

Location determines not only the climatic condition but also the structural loads that the structure must withstand. Given the broad variety of climatic and seismic requirements of Chile, the design of lightweight timber buildings considering both energy and seismic design parameters and boundary conditions becomes a difficult task. The main objective of this research is to analyze and quantify the effect of climates, seismic loads, lateral anchorage, and story number on the optimal energy design solutions, including the seismic behavior in a light-frame timber building. Furthermore, the optimal design was parametrically analyzed considering five Chilean cities that consider different climates, seismic zone, number of stories, and lateral anchorage systems to prevent rocking (overturning) due to lateral seismic forces. The optimal wall insulation thickness, stud spacing, and thermal mass exhibited significant variations depending on the buildings' number of stories, lateral anchorage system, climate, and seismic zone. Therefore, the results of this investigation reinforce the necessity of integrating energy and seismic designs for light-frame timber buildings. The optimal designs obtained in this investigation showed considerable variations depending on the combination of climatic and seismic loads as well as the number of stories and anchoring systems. The article's main contributions are the evidence of the structural and energy design interconnection of light-frame timber buildings and how design variables, such as stud spacing, floor concrete thickness layer, and wall insulation thickness, are related and change according to the different climates, seismic loads, lateral anchorage, and story number.

1 Introduction

The energy efficiency design of buildings can be influenced by many parameters such as fenestration characteristics like window wall rate (WWR), solar heat gain coefficient (SHGC), and window thermal transmittance (U_w) (Ahn et al. 2016; Feng et al. 2017; Yang et al. 2015), the materials of the building envelope (Mahar et al. 2020; Mirrahimi et al. 2016; Thomas and Ding 2018), HVAC system (Anna Chatzopoulou et al. 2016; Li et al. 2018), and thermal mass (Reilly and Kinnane 2017), among other parameters. Also, boundary conditions such as climate or internal heat gains affect the building energy design. Building energy optimization allows for dealing with the large number and complex interactions of energy-efficiency-related design parameters and boundary conditions to optimize the building energy performance, becoming an essential design approach to increase the buildings' energy efficiency (Harkouss et al. 2018).

Sayadi et al. (2021) optimized the WWR considering the HVAC and lighting energy consumption, different window configurations, and thermal comfort of the building for seven different climates. The authors performed the analysis in three southern, western, and eastern orientations, with the following three cases: the application of automated lighting control, the utilization of windows' horizontal overhang, and the application of automatic blinds to control solar heat gains. They concluded that for warmer climates the shades

✉ Pablo Guindos
pguindos@uc.cl

1 Centro Nacional de Excelencia Para La Industria de La Madera (CENAMAD), Pontificia Universidad Católica de Chile, Av. Vicuña Mackenna 4860, Santiago de Chile, Chile

2 Department of Construction Engineering and Management, Pontificia Universidad Católica de Chile, Av. Vicuña Mackenna 4860, Santiago de Chile, Chile

3 UC Energy Research Center, Pontificia Universidad Católica de Chile, Av. Vicuña Mackenna 4860, Santiago de Chile, Chile

4 Center for Sustainable Urban Development (CEDEUS), Pontificia Universidad Católica de Chile, Santiago de Chile, Chile

5 Department of Mechanics of Continuous Media and Theory of Structures, School of Architecture, University of A Coruña, 15071 A Coruña, Spain

Published online: 03 May 2024

or blinds are effective in reducing the energy consumption in the different window configurations, and the WWR optimal values were reduced compared to the colder climates to reduce solar heat gains. Otherwise, they found that no blinds or shades were implemented during the whole year in colder climates. Also, they observed a wider range of optimal WWR in colder climates. Vera et al. (2017a, b) performed an optimization on fixed exterior complex fenestration systems to improve both visual comfort and energy performance. They used a hybrid genetic algorithm to explore different configurations of the exterior complex fenestration, considering factors such as daylight autonomy, glare index, and energy consumption. Their results showed that it is possible to achieve a balance between visual comfort and energy efficiency through careful optimization of the exterior complex fenestration system design. Jia et al. (2021) studied the application of phase change materials (PCM) on prefabricated constructions to obtain optimal energy savings in five climates in China. They obtained different energy savings depending on the PCM's location and climate analyzed. For example, adding PCM into the walls and roofs in cold climates achieves energy savings of 17.7% and 14.5%, respectively. In mild climates, the impact of PCM is more significant with reductions of 77.1% and 67.5% for PCM located in walls and roof respectively. Ascione et al. (2019) performed a multi-objective optimization to find optimal solutions that produce the Pareto minimization of primary energy consumption, global cost, and discomfort hours in four Italian climates. The study was performed under two approaches: the nearly zero-energy buildings and a cost-optimal approach that minimizes the general costs. Their Pareto curve showed an interaction between the energy-efficient optimal and the cost-optimal in the different climate zones. Delgarm et al. (2016) proposed a methodology for the optimization of building energy efficiency in Iran to evaluate the capability and effectiveness of the methodology in a single room optimizing several parameters such as the building orientation, the shading overhang dimensions, the window size, and the glazing and the wall material properties regarding building energy consumption. As expected, different climates showed a considerable effect on energy consumption. For example, the optimum cooling energy consumption increased from 1 to 5.43 GJ, and the optimum heating energy consumption decreased from 12 to 2.2 GJ from cold to warm climates (Delgarm et al. 2016). The literature agrees that optimal building energy design is highly affected by climate, especially in residential buildings that show low internal heat gains.

The geographical location not only defines the climatic conditions in a building's energy optimization but also plays a crucial role in defining structural requirements such as snow, wind, and seismic loads. Especially the latter becomes critical in earthquake-prone regions for light-frame timber buildings because the lateral stiffness of this kind of building is remarkably lower than other structural systems such as reinforced concrete buildings. For example, lateral inter-story drifts often become the governing structural design parameter (Alarcón et al. 2023). A few authors investigated the integration of building energy performance under different seismic conditions. Pohoryles et al. (2020) simulated the effect of the building renovations for structural retrofitting and energy performance under a monetary metric called expected annual loss, which considered the energy consumption and the utilization of fragility curves for the expected damages under a seismic hazard. Twenty European cities located in areas of different climatic conditions and seismic hazards were studied. When using a combined annual loss, significant improvements leading to average reductions of at least one category in terms of combined seismic and energy classes for the residential building studies cases were obtained. Nevertheless, this study only focused on renovating the walls regarding thermal insulation, maintaining all other envelope characteristics such as fenestrations, thermal mass, etc. A similar study was performed by Manfredi and Masi (2018), as they assessed the influence between the seismic performance of infill masonry wall retrofitting techniques in residential buildings and the related energy reductions for each improvement. They identified the most common climates and compared the seismic capacity and hazard demand for the different seismic intensity levels. Their study presented two different rehabilitation configurations, first replacing the external layer with a new improved panel with better thermal insulation properties, and secondly, adding a reinforcement concrete frame to the existing structure similar to a double skin façade. They concluded that reductions up to 31 kWh/m^2·year were feasible under the first rehabilitation configuration and still achieved an improvement in seismic performance.

The interaction of energy and seismic requirements may become even more relevant for timber buildings. For instance, timber buildings typically weigh one to two-thirds the weight of concrete buildings, which reduces the thermal inertia, thus increasing the overheating risk (Dietz et al. 2020; Guindos 2019). The light weight of timber buildings accentuates the relative importance of the non-structural elements' weight on the building's seismic mass such as the materials' weight used for the building thermal and acoustic insulation or additional layers for increasing thermal mass (for example incorporating phase change materials, concrete floor topping layer). Guindos (2019) reported that adding a concrete topping layer on slabs to improve the thermal inertia of light-frame timber buildings can increase up to 40% of the seismic mass and the structural forces that the building must withstand. In addition, the low lateral stiffness of timber frame buildings requires high-density shear walls to comply with structural

building codes with maximum inter-story drifts (Berwart et al. 2022; Casagrande et al. 2012; Tomasi et al. 2015; Ugalde et al. 2019). Such requirement of high-density shear walls also constitutes a design trade-off with other design variables such as the windows openings for energy and visual comfort. Furthermore, it is essential to prevent the overturning or rocking of timber buildings under the action of lateral loads. Despite the shear walls providing enough lateral stiffness to be code-compliant, lateral drifts may exceed limits by just the overturning of shear walls. The amount of overturning is significantly larger in slender wall segments in comparison with long segments. In addition, overturning is also strongly affected by the number of stories. Thus, more stories cause larger overturning moments (Berwart et al. 2022). In timber buildings, overturning is prevented by installing lateral connector systems (anchorages) that restrain the uplift at the ends of shear walls as shown in Fig. 1 for typical light-frame timber shear wall configurations. Two of the most used anchorage systems consist of the continuous steel rod system

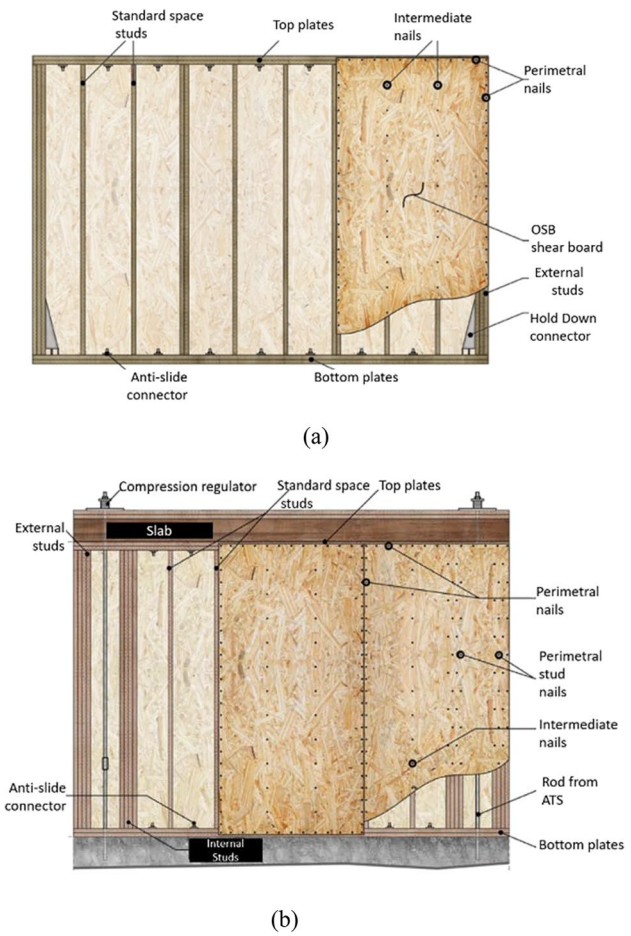

Fig. 1 Typical configuration of light-frame timber shear walls including two distinct anchorage systems (Wenzel et al. 2022): **a** Hold Downs connector. **b** ATS connector

(ATS) and the discrete hold-down systems (HD). The ATS system is typically stronger and stiffer than discrete hold-down systems but it is significantly more expensive, and therefore becoming a critical aspect of the buildings' design (Bagheri and Doudak 2020; Estrella et al. 2021).

In summary, the interaction aspects of the energy and seismic design in light-frame timber buildings typically included the building mass and the shear wall participation. These two characteristics influence the window openings, overturning risk due to increment in story numbers, and selection of lateral anchorage systems.

Despite the strong energy-seismic design interaction, the optimization of both aspects has been scarcely investigated in timber buildings. Only Polastri et al. (2016) analyzed the increment of thermal inertia and its effect on the structural and thermal performance of Cross Laminated Timber and light-frame timber buildings under different connectors for three and five stories. This study was part of an Italian project called *TIMBEEST*, in which the structural and energy performances were simulated in the second and third phases of the project. The project's second phase consisted of a parametric structural analysis of the connectors, number of stories, and improvement of walls according to Eurocode 8 (EN 1998–1 2004) and an elastic horizontal ground acceleration response spectrum variation. The structural results were considered for energy analysis, and a parametric study was performed using TRNSYS (Klein 1976) for both constructive systems and different window configurations considering WWR, SHGC, area, and U-value. Different thermal properties were improved for the increment in the thermal inertia of the building, such as thermal transmittance, periodic thermal transmittance, time shift, decrement factor, internal areal heat capacity, and long-term thermal capacity. Polastri et al. (2016) concluded that the mass increment in both construction systems was feasible in three stories for all Italian seismic zones. Whereas, the mass increase in walls could be accomplished only in zones with low earthquake risk in five-story buildings (Polastri et al. 2016).

As mentioned in the literature, the passive energy design of buildings and structural loads is affected by the locations, and energy-seismic designs strongly interact with each other, especially in timber buildings due to their inherent lightweight and low lateral stiffness. The research on the interaction of the structural and energy behavior in buildings is low, especially on how the design location can affect the design variables of a timber building. Therefore, the main objective of this research is to analyze and quantify the effect of climates, seismic loads, lateral anchorage, and story number on the optimal energy design solutions, including the seismic behavior in a light-frame timber building. This will allow a better understanding of the linkage among the energy and structural design parameters and how they affect the optimal solutions of lightweight timber-frame multifamily buildings.

Although our study is conducted at a national level, given the broad climatic and seismic conditions of the country, 25 types of climates (Sarricolea et al. 2017), three seismic zones from 0.2 g up to 0.4 g design accelerations, and six types of soil quality according to the Chilean standard NCh 433 (INN 1996), our results and conclusions provide a valuable insight into the international community of how relevant this interaction becomes in timber buildings. The optimization process was conducted based on a previous optimization model published by the authors, which details are briefly explained in the following section. Still, all the implementation details are found in Wenzel et al. (2022).

2 Energy and structural timber building model and optimization methodology

2.1 Overview of the overall procedure

The model and overall computational methodology applied to simulate both the energy and the structural behavior are found in Wenzel et al. (2022). This work proposed an Energy and Structural Timber Building Optimization (ESTIBO) model that allows to optimize the energy performance of a timber building considering the structural feasibility of the optimal solution. The mentioned framework simulates the energy behavior in EnergyPlus under the Honeybee plugin from Grasshopper, while the structural behavior was based on modal analysis and performed according to the Chilean standard for buildings' seismic design NCh 433 *Earthquake-resistant design of buildings* (INN 1996). The optimization process was performed via GenOpt with a hybrid algorithm Particle Swarm Optimization through a Constriction Coefficient and the application of the Hooke Jeeves with a Generalized Pattern Search algorithm (GPSPSOCCHJ). Finally, the model was applied in a residential light-frame timber building case study considering different stories, lateral connectors, and cities. All input parameters are detailed in the following sections.

2.2 Climates and seismic zones

Five cities representing different climates in Chile were selected for the design by optimization of the light-frame timber building. Table 1 shows each city's Köppen-Geiger climate classification, the ASHRAE climate classification, maximum, minimum, and average dry bulb temperatures, and solar radiation from the EPW files (Sarricolea et al. 2017; Todd 2003; Vera et al. 2017a, b). Table 2 shows the cities' latitudes, longitude, and elevation. A 10.32 °C decrease in the mean temperature was observed from the north to the south of Chile. Concerning the solar radiation in the cities, Escobar et al. (2015) concluded that a decrease

Table 1 Cities and climate classification

City	Köppen-Geiger	ASHRAE	Chilean thermal regulation	Maximum Dry Bulb Temperature (°C)	Minimum Dry Bulb Temperature (°C)	Average Dry Bulb Temperature (°C)	Annual Direct Normal Radiation (kWh/m^2)	Annual Diffuse Horizontal Radiation (kWh/m^2)	Global Horizontal Radiation (kWh/m^2)	Seismic Zone
Antofagasta	Csb	3A	A	25.2	7.0	16.6	1276.4	983.8	1771.3	Z3 (0.4 g)
Santiago	Bsk	4B	D	33.2	-6.0	14.4	1632.1	649.5	1791.0	Z2 (0.3 g)
Concepción	Csb	3C	E	29.0	-1.0	12.9	1244.2	816.0	1493.2	Z3 (0.4 g)
Puerto Montt	Cfb	4C	H	27.0	-3.1	10.4	594.0	742.2	1047.8	Z2 (0.3 g)
Punta Arenas	Cfc	4C	I	22.0	-6.0	6.3	569.0	666.6	898.9	Z2 (0.3 g)

Table 2 Latitude, longitude, and elevation of the cities

City	Latitude	Longitude	Elevation(m)
Antofagasta	-23.64637	-70.39800	14.0
Santiago	-33.43778	-70.65045	574.0
Concepción	-36.82708	-73.05024	36.0
Puerto Montt	-41.47181	-72.93962	15.0
Punta Arenas	-53.16257	-70.90782	17.0

in Global Horizontal Radiation (GHR) and Direct Normal Radiation (DNR) could be observed in coastal cities due to the persistence of seasonal cloud covers with daily cycles. Only Santiago is settled in a noncoastal area, presenting the highest GHR and DNR among the chosen five cities.

Further to the climatic constraints, the location also defines the seismic design acceleration and soil quality. The city location affects the effective acceleration according to the Chilean seismic code NCh 433 *Earthquake resistant design of buildings* (INN 1996), in which the seismic intensity is divided into three categories from lesser to higher accelerations: the Andes mountain area (labeled as Z1 and with a design acceleration of 0.2 g), the central area (Z2, 0.3 g), and the coastal area (Z3, 0.4 g). The acceleration increase depends on the distance to the shallowest portions of the South American subduction zone. For example, the coastal regions show the highest effective acceleration value (Rojas et al. 2010). Regarding soil quality, the NCh 433 standard categorizes 6 levels of decreasing quality from A to F. In all study cases, the soil quality presented a B classification according to the Chilean seismic standard. Seismic acceleration and soil quality affect the lateral strength vector for the modal analysis.

The structural performance model was constructed based on the following procedures:

- The shearwall lateral capacity and stiffness were calculated according to the *Special Design Provisions for Wind and Seismic of the United States of America* (SDPWS, American Wood Council 2014).
- The calculations of each timber frame element (posts and beams) and connections of the building were carried out according to the NCh 1198 *Wood — Wood construction — Calculation* (INN 2014), which in many sections is concordant with the allowable stress design methodology prescribed in the National Design Specification of the United States of America (NDS 2015) for the calculation of dimensional lumber, timbers, and joists, as well as lateral connectors.
- The determination of the seismic forces and modal analysis was based on the NCh 433 *Earthquake-resistant design of buildings* (INN 1996), which prescribes a modal combination procedure based on the vibration modes of the structure that were dependent on the building weight and stiffness.
- The capacity and stiffness of the anchorage systems (HD and ATS) were based on the values given by the manufacturer (Simpson Strong Tie Co Inc, Pleasanton, CA, USA). Table 3 shows the connector's properties.

The verification of failure modes of the structural elements included the shear failure of the wall boards (SB) or sheathing, compression strength of the end studs (CES) or shear wall chords, compression strength of the internal studs (CIS) only for the ATS anchorage system, compression strength of the standardly spaced studs (CSS), tensile failure of lateral connectors or anchors (TLC), and tensile failure of the end studs (TES) or shearwall chords. The shearwalls were automatically selected from the energy model as those wall segments with lengths equal to or larger than half the shearwall height.

2.3 Energy model

The energy model was constructed in Rhino via Grasshopper and the Honeybee plugins. Honeybee performs the buildings' energy simulations through EnergyPlus. The energy simulation parameters, zone assumptions, and materials properties used are similar to the study of Wenzel et al. (2022). The simulation parameters from EnergyPlus are illustrated in Table 4. The windows were considered as a "Simple Window Elements" that are characterized by the U-value (U_w) and a SHGC factor.

Table 3 Connector properties

Anchorage type	Commercial Model	Net Area (cm^2)	Admissible Tension (KN)	Failure stress (N/mm^2)
HD	12	2.22	29.22	-
HD	26	2.54	72.08	-
ATS	0.75	2.16	-	826.73
ATS	1.25	5.99	-	826.73
ATS	1.75	12.25	-	826.73

Table 4 EnergyPlus simulation parameters

Simulation parameters	Value	Unit
Cooling setpoint	25	°C
Heating setpoint	20	°C
Air change per hour	1	h^{-1}
Equipment and lighting heat gains	24.5	W/m^2
People heat gains	3	W/m^2
Ventilation rate	0.0075	m^3/s

A light-frame timber wall can be considered a non-homogeneous element, with the studs acting as thermal bridges. To take into account the effect of the thermal conductivity of the wall structural elements and the presence of thermal bridges on the thermal transmittance was calculated according to the ISO 6946 *Building Components and building elements -Thermal Resistance and Thermal Transmittance—Calculation Methods* (ISO 2017). In the case of opaque surfaces, the thermal properties of their elements are shown in Table 5. The table shows constant and non-constant values depending on the property if it was a design variable in the optimization problem. Table 6 shows the input values implemented in the optimization problem. It should be noticed that the wall insulation type was a property added as a discrete variable to choose between two insulating materials that show a contrast in thermal mass-related properties, the insulation variables were added as a discrete value of 1 and 2. Table 7 shows the thermal properties considered for the wall insulation materials.

2.3.1 Optimization process

GenOpt (Wetter and Gov 2016) performed the optimization with the GPSPSOCCHJ algorithm and a static death penalty. Table 8 shows the optimization parameters used in this investigation.

In the case of the hold-down optimization problem, the particle number increased to 30 individuals. This increment was based on the highly penalized first generation that could cause inefficient work if the initial particles did not search the space correctly in the PSO algorithm (Digehsara et al. 2020). The optimization variables deemed in this study are presented in Table 9. The Chilean Draft Standard Ntm11-2 (OGUC 2014) provides different minimal thermal resistance values for the wall, roof, and ground floor elements. Therefore, different lower limits were assigned to each of these variables during optimization to satisfy the Ntm11-2 thermal standard. Table 10 shows the optimization variables with the corresponding minimum for the cities analyzed.

The optimization objective function seeks to minimize the sum of the thermal loads with a penalty function related to the structural performance. The penalty function was applied if the building's lateral drift limits in the X and Y directions surpassed the limit conditions and if any wall's utilization factor (UF) was over 1. The UF was defined as the relationship between the structural failure modes forces to withstand and the capacity available. The objective and penalty functions are presented in Eqs. 1 and 2, respectively. The variables of $heating_i$ and $cooling_i$ represent the thermal loads for the i zone of the building. The index i represents the conditioned space, and N the total spaces conditioned.

$$F_{obj} = min\left(\sum_{i=1}^{N}(heating_i + cooling_i\right) + Penalty) \quad (1)$$

$$Penalty = \begin{cases} 0 & if(max\ (UF) \le 1) \wedge (Drift\ X, Y) \le 0.002 \\ \frac{50000}{Conditioned\ Area} & otherwise. \end{cases} \quad (2)$$

2.4 Total of case studies in the optimization problem

Table 5 Dimensions and thermal properties of roof, floors and walls design variables

	Dimension (mm)	Thermal conductivity (W/m K)	Density (kg/m^3)	Specific heat (J / kg K)	Stud spacing (mm)
Roof insulation	Variable	0.042	40	6700	-
Wall insulation	Variable	Mineral wool*/Wooden Fiber Insulation*			-
Ground floor insulation	Variable	0.0361	40	1300	-
Floor concrete thickness layer	Variable	1.63	2400	1000	-
Wall stud cross-section	41 × 138	0.156	513	1200	Variable

*see Table 7 for the properties

Table 6 Thermal properties of the wall insulation materials

Insulation type	Conductivity (W/m K)	Density (kg/m^3)	Specific heat (J / kg K)
Standard insulation—mineral wool (1)	0.042	40	6700
Heavy insulation—wooden fibers insulation (2)	0.040	190	2100

The case study considered in this investigation consists of a light-frame timber residential building in four, five, and six stories with different anchorage systems. The building comprises four apartments per floor, measuring 95.7 m^2 each. The conditioned zones represent 77.4 m^2 of the apartment area. The location of the case study was variable depending on the cities analyzed. The design methodology was applied to four, five, and six-story light-frame timber buildings to investigate different optimal building configurations and the interactions among structural and energy design parameters. Figure 2 illustrates the four-story case.

Table 7 Optimization parameters

Optimization parameters	Value
Neighborhood Topology	Von Neumann
Number of Particles	10
Maximum Number of Generation	10
Cognitive Acceleration	2.8
Social Acceleration	1.3
Maximum Velocity Gain	0.5
Maximum Velocity	4
Constriction Gain	0.5
Mesh Size Divider	2
Initial Mesh Size Exponent	0
Mesh Size Exponent Increment	1
Number Of Step Reduction	3

The number of case studies corresponded to a combination of lateral connectors, design locations, and stories. This research carried out a total of 20 optimization problems, and there was no structural feasibility in the five and six-story building cases with the hold-down connector due to its low capacity, leading to an unfeasible structural solution. The distribution of the lateral connectors depends on the number of stories. For instance, the lower stories require stronger anchorages than the upper stories due to larger overturning moments. Table 11 presents the lateral connector combination for the different building stories.

3 Results and analysis

The results and analysis sections are presented in different subsections. First, the optimization results are shown, including an analysis of the WWR, roof insulation thickness variables, and the high penalty case studies. The second subsection analyses the climate effect on the optimal solutions. Subsequently, the effect of the seismic zone on the optimal results is presented. Finally, an analysis of the mass balance, the effect of anchorages, and the number of stories is discussed.

3.1 Optimization outputs

Table 12 shows the cooling and heating loads and governing structural failure modes of all the analyzed cases, while Fig. 3 shows the optimal values of optimization variables for all the optimization problems. The optimal variables present minor differences affected by the number of stories and lateral anchors, showing similar energy loads for each city.

The optimal energy performance outputs, heating and cooling loads achieved different values according to the climate of the case studies. The structural performance was highly dependent on the seismic zone and story number. For example, Antofagasta presented higher cooling loads than heating loads. Regarding the structural performance, due to the higher seismic acceleration and the increment of the seismic loads, shear of the wall board (SB) was the predominant structural failure mode, except for the four-story hold-down (HD) cases, which presented a tension of the lateral connector (TLC) failure mode because of the lower lateral connector capacity. Santiago showed a balanced distribution of energy loads and more diverse structural failure mechanisms because it was affected by lower seismic demand. The failure modes presented were TLC, SB, and compression of the standardly spaced studs (CSS). Concepción climate has a lower mean dry bulb temperature than Santiago and Antofagasta and less extreme temperatures than Santiago, showing higher heating than cooling loads but still lower energy loads than Santiago. The structural failure distribution in Concepción is similar to the buildings located in Antofagasta. Punta Arenas and Puerto Montt present higher heating requirements due to the lower temperatures and solar radiation. Building cases in both cities exhibited similar structural failure modes to Santiago.

3.2 Optimization variables

Regarding the optimization variables, the optimal value depended on the climate and/or seismic zones. Still, two variables showed the same optimal value for all optimization problems: the WWR and roof insulation thickness, with values of 0.3 and 240 mm, respectively. The literature shows that improving occupants' thermal comfort and reducing the energy performance of buildings require WWR lower than 50% (Alghoul et al. 2017; Cesari et al. 2018; Goia et al. 2013; Lam et al. 2015; Lee et al. 2013; Marino et al. 2017; Uribe et al. 2018; Xue et al. 2019). Moreover, WWR should be low even with low SHGC values (Uribe et al. 2018). In warm climates, the optimal WWR of 0.3, which is the lowest value that can be selected by the optimization algorithm, agrees well with the findings of previous researchers. From the structural standpoint, increasing the WWR reduced the perimetral shear walls and, consequently, the building's lateral stiffness and capacity. This reduction typically yielded higher deflection under the seismic loads and increased the risk of SB and anchorage failure modes. Therefore, the lowest WWR in all climates and seismic zones contributes significantly to obtaining a better energy and structural performance of the analyzed buildings.

The roof surface was susceptible to high solar radiation and air temperature in Antofagasta, Santiago, and Concepción. Instead, Puerto Montt and Punta Arenas show lower mean temperatures and solar radiation than the rest of the cities. Therefore, the roof surface insulation may reach a higher or maximum value to minimize the heat gains or losses, depending on the climate. The roof insulation was not considered as a material that added weight to the structural simulation, thus, there was no structural influence in the optimal selection.

Table 8 Optimization variable range

Variable to optimize	Maximum Value	Initial Value	Step Value
Window Wall Rate (%)	0.8	0.5	0.05
Windows thermal transmittance (W/ m^2 k)	2.7	2.2	0.1
SHGC (-)	0.8	0.6	0.05
Wall insulation thickness (mm)	200	120	10
Roof insulation thickness (mm)	240	140	10
Ground insulation thickness (mm)	80	35	5
Concrete layer thickness (mm)	120	70	10
Wall insulation type (-)	2	1	Discrete
Stud Spacing (mm)	600	400	Discrete

Table 9 Optimization variables and minimal values

Thermal Zone According Regulation	Minimal values for optimization				
	A	D	E	H	I
City	Antofagasta	Santiago	Concepción	Puerto Montt	Punta Arenas
Window Wall Ratio (%)	0.3	0.3	0.3	0.3	0.3
Windows thermal transmittance (W/ m^2 k)	1.6	1.6	1.6	1.6	1.6
SHGC (-)	0.3	0.3	0.3	0.3	0.3
Wall insulation thickness (mm)	40	40	60	160	130
Roof insulation thickness (mm)	40	110	130	190	190
Ground insulation thickness (mm)	10	20	20	35	35
Concrete layer thickness (mm)	10	10	10	10	10
Wall insulation type (-)	1	1	1	1	1
Stud Spacing (mm)	300	300	300	300	300

3.3 High penalty case studies

The four-story HD building, six-story ATS building, and all buildings in the seismic zone 3 (stronger accelerations) were subjected to heavy structural penalizations. For example, the penalty of Eq. 2 was frequently applied in the PSOCC search, which may affect the optimal selection of discrete variables like stud spacing and wall insulation type. For instance, in the four-story HD problem in Punta Arenas, the stud spacing optimal value was set as 300 mm. Table 12 shows that the predominant structural failure mode in this case, was TLC, leading to an oversized solution. The 300 mm stud spacing shall increase the wall thermal transmittance value and the floor concrete thickness layer in contrast to what is observed in the seismic zone 2 four-story cases. This circumstance misleads the PSO optimal value by selecting discrete variables that satisfy the structural requirements but do not reach the optimal value for energy reductions. According to GenOpt (Wetter and Gov 2016), after the PSO algorithm finishes the local finding of the global optimum, a local search is performed by the HJ algorithm (Hooke and Jeeves 1961) with adaptive precision function evaluations using the model GPS algorithm. In this local search, the algorithm fixes the discrete variables and cannot change their value in the local verification. Moreover, the misleading of the algorithm led to the selection of new local optimal points for these variables, searching for the lowest objective function with the second part of the algorithm.

Table 10 Lateral connectors' commercial model and distribution

Number of Stories	Floor	ATS Size	HD Size
4	1	1.75	26
	2	1.75	26
	3	0.75	12
	4	0.75	12
5	1	1.75	-
	2	1.75	-
	3	1.25	-
	4	0.75	-
	5	0.75	-
6	1	1.75	-
	2	1.75	-
	3	1.25	-
	4	1.25	-
	5	0.75	-
	6	0.75	-

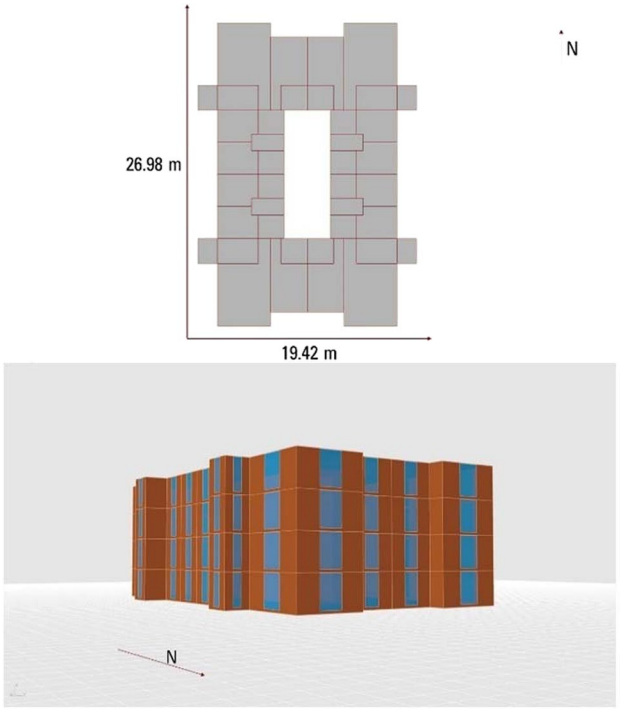

Fig. 2 Floor plan (top) and perspective view of the four-story case study (bottom) (Wenzel et al. 2022)

Table 11 The cooling and heating loads, and governing structural failure modes for the studied cases

City	Anchor	Heating (kWh/m^2)	Cooling (kWh/m^2)	Structural failure mode
Antofagasta (Csb-3A)	4 Story HD	3.2	16.1	TLC
Antofagasta (Csb-3A)	4 Story ATS	2.8	15.7	SB
Antofagasta (Csb-3A)	5 Story ATS	3.0	16.0	SB
Antofagasta (Csb-3A)	6 Story ATS	2.8	16.5	SB
Santiago (Bsk-4B)	4 Story HD	21.7	19.9	TLC
Santiago (Bsk-4B)	4 Story ATS	21.3	19.4	CSS
Santiago (Bsk-4B)	5 Story ATS	20.7	20.1	SB
Santiago (Bsk-4B)	6 Story ATS	20.4	20.6	CSS
Concepcion (Csb-3C)	4 Story HD	18.6	12.5	TLC
Concepcion (Csb-3C)	4 Story ATS	17.0	12.2	SB
Concepcion (Csb-3C)	5 Story ATS	17.1	12.4	SB
Concepcion (Csb-3C)	6 Story ATS	18.4	11.8	SB
Puerto Montt (Csf-4C)	4 Story HD	30.5	11.4	TLC
Puerto Montt (Csf-4C)	4 Story ATS	29.3	11.4	CSS
Puerto Montt (Csf-4C)	5 Story ATS	28.4	12.0	SB
Puerto Montt (Csf-4C)	6 Story ATS	29.4	11.3	CSS
Punta Arenas (Cfc-4C)	4 Story HD	55.0	12.2	TLC
Punta Arenas (Cfc-4C)	4 Story ATS	53.5	11.8	CSS
Punta Arenas (Cfc-4C)	5 Story ATS	53.0	11.9	SB
Punta Arenas (Cfc-4C)	6 Story ATS	53.0	12.2	CSS

3.4 Effect of climates on the optimal solutions

The effect of the climate is remarkable in the resulting optimal solution for the different cities as they change from warm climates such as Antofagasta to cold climates like those of Punta Arenas. For example, Fig. 3 shows a progressive reduction of U_w from 2.7 W/m^{2}k to 1.6 W/m^{2}k from warm to cold climates. The SHGC varied similarly, with a gradual increment from 0.3 to 0.8 from warm to cold climates. The ground insulation thickness ranged from 15 mm for Antofagasta to 80 mm in Puerto Montt and Punta Arenas. Therefore, the optimization procedure found the optimal values of these design variables according to the climate conditions.

In almost all studied cases, regardless of the insulation type, the wall insulation thickness reached a high value, confirming the wall insulation's positive effect in reducing the thermal loads for all climates. However, the algorithm selected intermediate values for the wall insulation thickness to balance the heat gains and heat losses through the wall in Antofagasta, which presents the highest radiation and mean dry bulb temperature.

3.5 Seismic effect on the optimal solutions

The effect of the seismic zones was highlighted on the variables that increase the light-frame timber building mass and shear wall performance. The seismic zone conditioned the optimal wall insulation thickness, the floor concrete layer thickness, stud spacing, and wall insulation type.

In cities with the most intense seismicity, Antofagasta and Concepción, the mass addition was an essential parameter due to the remarkable increment of the lateral design forces. The structural failure modes and the floor concrete thickness layer were strongly conditioned. The SB was the dominant structural failure mode in all the ATS anchors of seismic zone 3. The failure mode of the four-story HD in all case studies was the TLC. Another variable that was highly affected by the seismic zone and increased the building mass was the floor concrete layer thickness. Figure 3 shows a thinner concrete layer in almost all case studies of seismic zone 3 compared to seismic zone 2. However, there is an exception on the four-story ATS due to the low total building height and lateral connector capacity, in which the lateral forces were lower than the five and six-story buildings and the connector capacity was higher than the HD. This led to a similar floor concrete layer thickness independent of the seismic zone. These results indicate that in zones with high seismic acceleration, the high mass components in the light-frame timber building, such as the floor concrete layer topping, were limited and reduced compared to the cities with a lower seismic acceleration. This is confirmed by the results of building cases in seismic zone 2, as they present lower seismic acceleration and achieve thicker floor concrete

Table 12 Relationship of WWR, concrete floor thickness, and wall U-value regarding climate and structural behavior

City	Building stories and connector type	Climate	Seismic Zone	Optimal WWR constrained by climate	Optimal WWR constrained by structural performance	Stronger building structural design due to optimal WWR	Optimal concrete floor thickness constrained by climate	Optimal concrete floor thickness constrained by structural performance	Stronger building structural design due to optimal concrete floor thickness	Optimal wall U-value constrained by climate	Optimal wall U-value constrained by structural performance	Stronger building structural design due to optimal wall U-value
Antofagasta	4 Story HD	Csb-3A	Z3 (0.4 g)	✓	No	✓	No	✓	✓	No	✓	No
Antofagasta	4 Story ATS	Csb-3A	Z3 (0.4 g)	✓	No	✓	No	✓	✓	No	✓	✓
Antofagasta	5 Story ATS	Csb-3A	Z3 (0.4 g)	✓	No	✓	No	✓	✓	No	✓	✓
Antofagasta	6 Story ATS	Csb-3A	Z3 (0.4 g)	✓	No	✓	No	✓	✓	No	✓	✓
Santiago	4 Story HD	Bsk-4B	Z2 (0.3 g)	✓	No	✓	No	✓	✓	No	✓	No
Santiago	4 Story ATS	Bsk-4B	Z2 (0.3 g)	✓	No	✓	No	✓	✓	✓	No	✓
Santiago	5 Story ATS	Bsk-4B	Z2 (0.3 g)	✓	No	✓	No	✓	✓	✓	No	✓
Santiago	6 Story ATS	Bsk-4B	Z2 (0.3 g)	✓	No	✓	No	✓	✓	✓	No	✓
Concepción	4 Story HD	Csb-3C	Z3 (0.4 g)	✓	No	✓	No	✓	✓	No	✓	No
Concepción	4 Story ATS	Csb-3C	Z3 (0.4 g)	✓	No	✓	No	✓	✓	✓	No	✓
Concepción	5 Story ATS	Csb-3C	Z3 (0.4 g)	✓	No	✓	No	✓	✓	✓	No	✓
Concepción	6 Story ATS	Csb-3C	Z3 (0.4 g)	✓	No	✓	No	✓	✓	✓	No	✓
Puerto Montt	4 Story HD	Csf-4C	Z2 (0.3 g)	✓	No	✓	No	✓	✓	No	✓	No
Puerto Montt	4 Story ATS	Csf-4C	Z2 (0.3 g)	✓	No	✓	No	✓	✓	✓	No	✓
Puerto Montt	5 Story ATS	Csf-4C	Z2 (0.3 g)	✓	No	✓	No	✓	✓	✓	No	✓
Puerto Montt	6 Story ATS	Csf-4C	Z2 (0.3 g)	✓	No	✓	No	✓	✓	✓	No	✓
Punta Arenas	4 Story HD	Cfc-4C	Z2 (0.3 g)	✓	No	✓	No	✓	✓	✓	No	✓
Punta Arenas	4 Story ATS	Cfc-4C	Z2 (0.3 g)	✓	No	✓	No	✓	✓	✓	No	✓
Punta Arenas	5 Story ATS	Cfc-4C	Z2 (0.3 g)	✓	No	✓	No	✓	✓	✓	No	✓
Punta Arenas	6 Story ATS	Cfc-4C	Z2 (0.3 g)	✓	No	✓	No	✓	✓	✓	No	✓

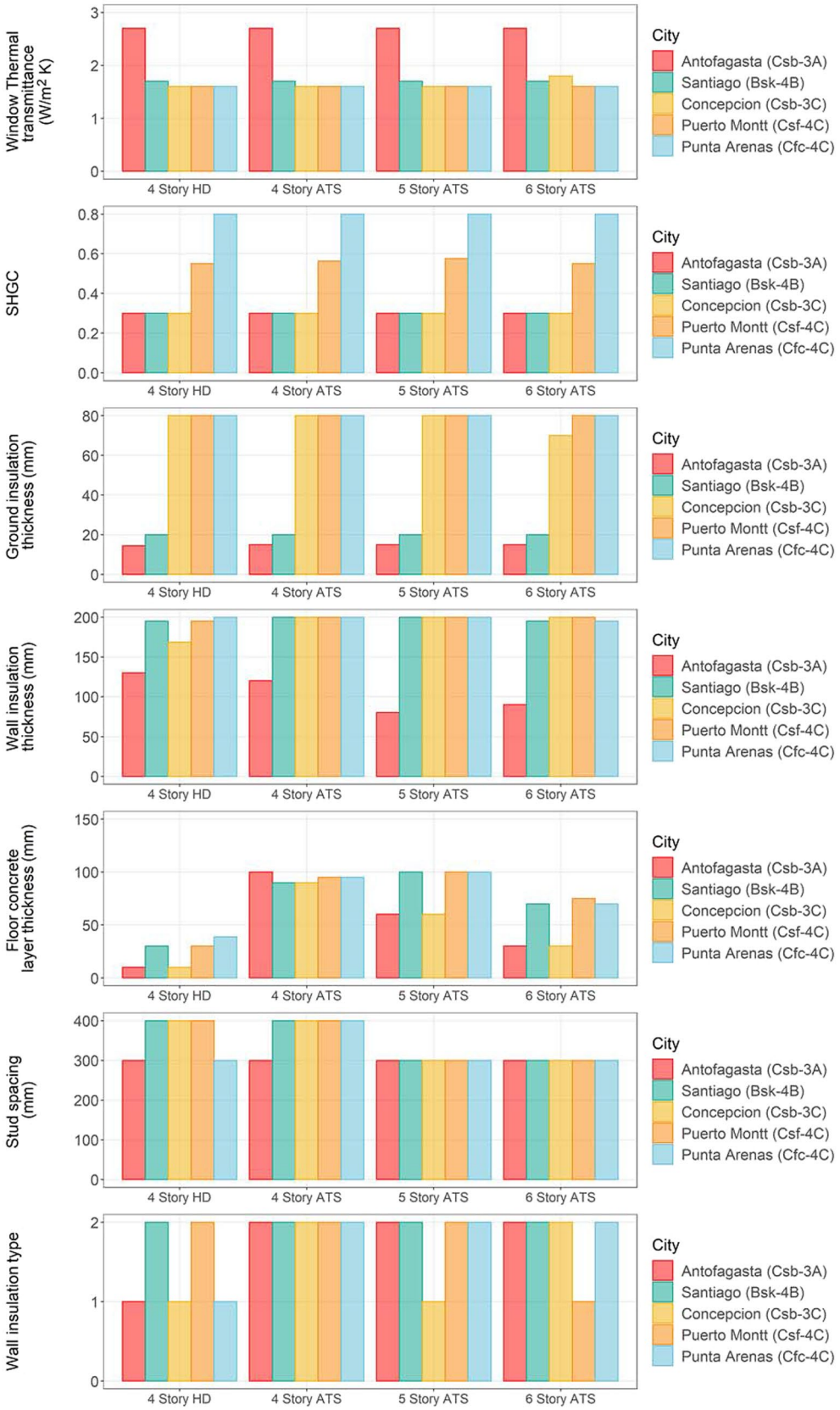

Fig. 3 Optimal design solutions for the studied cases

layers, from 100 to 70 mm, without reducing the wall insulation thickness. Moreover, the predominant structural failure was not only the SB but also the mass increment produced a compressive failure of the standard spaced studs (CSS).

3.6 Effect of mass balance, lateral connector, and number of stories

The impact of variables that add mass (for example: wall insulation thickness, stud spacing, and floor concrete layer thickness) was analyzed for all case studies to understand the mass quantity required to reach the optimal designs depending on the seismic zone, climate zone, heavy structural penalizations instances, story number, and lateral connector. The effect of the mass balance was clearer in some cases due to the difference in the final optimal design solution, for instance, comparing the four-story HD of Punta Arenas and Puerto Montt and the general cases of the six-story ATS. Punta Arenas and Puerto Montt four-story HD cases show climates highly dominated by heating loads but have different optimal discrete variables (i.e. wall insulation type, stud spacing) affecting the optimal value of the continuous variables. In the case of Punta Arenas, the wall insulation type and stud spacing in the four-story HD presented a misleading optimal value, reaching a 300 mm stud spacing and a lighter wall insulation type. A reduced stud spacing increases the building frame mass in contrast to lighter insulation, reducing the wall weight. This selection of discrete variables allows a thicker concrete layer of 38 mm and a maximum wall insulation thickness of 200 mm. Instead, Puerto Montt reached a 30 mm floor concrete layer thickness with a 195 mm wall insulation thickness with the heavier insulation alternative. In this case, the mass balance found different optimal solutions based on the discrete variables of stud spacing and wall insulation type. In the case of the six-story ATS buildings, they reached thicker wall insulation for all cities except Antofagasta. Due to the increase in building stories, the weight addition becomes critical for the first-floor stud compression capacity. Figure 3 shows that the wall insulation thickness reaches the maximum value in two of the five cities, being 195 mm in Santiago and Punta Arenas. On the contrary, the floor concrete layer thickness did not keep the minimum value, achieving a value in the range of 30 to 75 mm on the six-story ATS buildings. These results indicate that the algorithm prioritized the wall insulation thickness but still considered the benefit of thermal inertia granted by the floor concrete layer and performed a balance to obtain the optimal energy performance with a feasible structural solution.

A remarkable influence of the lateral connectors and the number of stories was found on the optimal designs. For example, the optimal solution for the four-story HD building was highly influenced by the lateral connector capacity and seismic zone. Figure 3 shows a notable difference in the optimal floor concrete layer thickness in all cities for the four-story buildings, evidencing reduced values due to the lower anchorage capacity and seismic zone. On the other hand, in the ATS buildings, the connector improved the lateral resistance of the light-frame timber building. It allowed incrementing both floor concrete layer and the wall insulation thicknesses. Concerning the wall insulation thickness and lateral connectors, in all cases (except Antofagasta) an attempt was noticed to maximize the value regardless of the lateral connector. These results evidence that the seismic zone and the lateral connector affect the optimal design, but there are still variables like the wall insulation thickness that reach high values in comparison to the others to minimize the thermal loads.

Regarding the number of stories on the four, five, and six-story ATS light-frame timber building, there was a direct effect on the stud spacing variable and the building mass of the optimal solution for the different cities. The optimal stud spacing was reduced according to the mass increment due to the rise of the story number. This reduction switched the stud spacing from 400 to 300 mm, increasing the walls' thermal transmittance and the building's frame mass. The additional concrete thickness decreased with the increment of the story number from 100 to 70 mm. The five-story building under seismic zone 2 achieved a thicker value of 100 mm on the floor concrete layer thickness due to the reduction of stud spacing. The story number highly conditioned the stud spacing to achieve a feasible structural solution considering the additional weight of the floor concrete layer and whole stories.

3.7 Discussion

The results and analysis presented previously evidence the effect of energy performance, structural performance, or both on the obtained optimal solutions. Most of the research is focused on the impact of climate and indoor heat gains (occupants, equipment and appliances, lighting) on the optimal solutions to achieve energy-efficient buildings. However, these analyses fail to consider the building's structural performance which could be affected by the energy-efficient design solutions. The above sections have shown the two-way impacts between energy efficiency and structural seismic parameters. Nevertheless, it is complex to understand in which cases the climate or the building structural performance constraints the optimal solutions because any change in the design parameters affects both domains and interactions propagate to other design parameters. In this section, we discuss how WWR, concrete floor thickness, and wall U-value are constrained by climate or structural performance and how climate's optimal solutions affect the building's structural design. Table 12 shows that the outdoor environment limits the optimum WWR in all cases, while the building structural performance restricts the optimum concrete floor thickness in all cases. For the wall U-value, some cases are determined by climate and others by structural performance.

The building's structural performance does not restrict the WWR because it is chosen at the minimum value to maximize

energy efficiency. However, having the lowest window area implies longer shear walls, reducing structural failure risk. Therefore, a WWR of 0.3 causes a more robust building structure. The concrete floor layer is required to increase the thermal inertia of the timber building to reduce the cooling energy loads significantly. In Santigo, Concepción, Puerto Montt, and Punta Arenas, the concrete floor thickness does not reach the maximum that would cause a more energy-efficient building. Therefore, in many cases, this design parameter is upper limited because the floor weight exceeds what the structural design can sustain. For example, in the case of 4-story buildings in Antofagasta with HD connectors, the optimal concrete floor thickness is the minimum (10 mm), which is reasonable due to very low cooling loads and because that was the maximum value that the 4-story HD in seismic zone 3 can achieve. Moreover, the algorithm added heavy insulation (type 2) in walls to get additional thermal mass and insulation at lower weight because the concrete floor thickness cannot be increased. In all cases of 5 and 6 stories, ATS connectors were needed to withstand the efforts caused by the concrete floor thickness and heavy wall insulation, besides the weight of having more stories.

Unlike WWR and concrete floor thickness, the climate defined the wall's insulation thicknesses in many cases. Nonetheless, there were also several cases in which this design parameter was limited by the structural performance constrained it. For instance, in the 4-story building with HD connectors, the wall's insulation thickness does not reach values close to the maximum despite being defined higher for Santigo, Puerto, and Punta Arenas. Here, the structural performance chose to reduce the wall's insulation thickness to avoid having a higher building weight that the structure could not support.

If the structural and seismic behaviors were not accounted for in the energy optimization of a light frame timber building in more demanding climates, some design parameters would reach non-feasible structure-seismic performance.

4 Conclusion

This research evaluated the effect of the different climates and seismic zones, story numbers, and lateral connectors in optimizing the energy behavior of feasible structural solutions for a light-frame timber building. The study contributes to the understanding of how the design variables of a light-frame timber building interact under different requirements defined by climates and seismic zones. The article focused on five different cities in Chile, representing a case study covering very distinct climates and seismic demands. An optimization procedure called ESTIBO was used to find the optimal thermal loads, granting a feasible structural design. The optimization objective function aimed to minimize the sum of the cooling and heating loads with a penalty function for cases where structural criteria were unsatisfied. Minimal values for the insulation thickness were set based on national building envelope insulating regulations. This model analyzed an optimized 20 cases, including buildings stories from four to six stories that used distinct anchoring technologies and a variety of climatic and seismic conditions. The novel analysis of the interactions between the seismic and energy on the optimal building design parameters allowed us to reach the following findings:

- The overall results evidenced the necessity of integrating both the energy and structural-seismic designs to obtain an optimal energy design that can achieve a feasible structural solution incorporating the different design parameters such as story number, lateral connector, and seismic zone. The interactions of both the energy and structural design variables were shown in the paper.
- The seismic zone characterized the structural failure mode depending on the lateral connector type and building stories. In addition, the floor's concrete thickness was reduced in seismic zone 3 (Antofagasta and Concepción) due to increased weight and lateral forces. These results indicate that the recommended floor concrete thickness for light-frame timber buildings to add thermal inertia to reduce building cooling loads must consider the building's seismic zone, stories, and lateral connector strength.
- The algorithm made a mass balance for all the cases to obtain the optimal energy designs with feasible structural solutions. These balances indicate that an analysis of the boundary values from the design variables has to be performed due to the possible combinations, such as story number, lateral connector, and seismic zone, which can achieve different energy outputs.
- The wall's insulation thicknesses were maximized in almost all optimization problems except in the warm climate of Antofagasta and the case of four-story HD in Concepción. The results show the positive effect of this variable on the thermal loads, independent of the type of insulation, story number, lateral connector, and seismic zone. Still, the seismic zone conditioned the optimal value on the wall insulation thickness in the four-story HD in Concepción, showing more clearly the interaction between the structural and thermal behavior.
- The WWR reached the minimal value of 0.3, reducing the thermal load and improving the building's lateral stiffness and capacity. The results show that a low WWR was the optimal solution, aligning both seismic and energy performance.
- The story number conditioned the stud spacing to resist the additional floor weight. A reduction from 400 to 300 mm stud spacing is chosen to withstand the increment of static and lateral loads in the five-story and six-story buildings. As expected, this reduction increased

the wall thermal transmittance and building frame mass but allowed for achieving the optimal solutions under heavier structural loadings was necessary.

- The cases of four-story HD buildings with high penalty problems, six-story ATS buildings, and all buildings in the seismic zone 3 presented misleading solutions based on the optimization procedure of the discrete variables. The misleading generates new local optimal solutions around the discrete variables.

Future research efforts should incorporate additional optimization decision-making parameters into the optimization framework during the building design stage, such as life cycle analysis (LCA), HVAC systems, and in-situ renewable energy generation systems, for the holistic design of optimized buildings. A multi-objective algorithm could be applied to integrate the LCA, HVAC and lighting systems, renewable energy on-site sources, and building envelope design variables. Moreover, the structural analysis might be set as an additional objective function. The advancement of the integrative optimization of such important design aspects should positively contribute to the achievement of more sustainable buildings that are optimized not only in terms of the operational energy but also in terms of the materials' embodied energy and demolition/recycling energy, as well as better tailoring the design of our buildings to the climatic change. This approach should lead to a much more controlled utilization of thermal mass and resources in the construction industry.

Acknowledgements The authors acknowledge the support of Chilean Agency or Research and Technology, the National Excellence Center for the timber industry CENAMAD (ANID BASAL FB210015) and the Center for Sustainable Urban Development CEDEUS (ANID/FONDAP 1523A0004).

Author contributions AW conducted the most details of the research as master student, he also drafted most of the parts of the paper. SV and PG co-supervised AW in his master, and provided the main conceptualization, funding, supervision and corrections of the paper.

Funding Open Access funding provided thanks to the CRUE-CSIC agreement with Springer Nature.

Data Availability Data availability of this research can be provided upon request.

Declarations

Competing interests The authors declare no competing interests.

References

Ahn BL, Kim JH, Jang CY, Leigh SB, Jeong H (2016) Window retrofit strategy for energy saving in existing residences with different thermal characteristics and window sizes. Build Serv Eng Res Technol 37(1):18–32. https://doi.org/10.1177/0143624415595904

Alarcón M, Soto P, Hernández F, Guindos P (2023). Structural health monitoring of South America's first 6-Story experimental light-frame timber-building by using a low-cost RaspberryShake seismic instrumentation. Eng Struct 275. https://doi.org/10.1016/j.engstruct.2022.115278

Alghoul SK, Rijabo HG, Mashena ME (2017) Energy consumption in buildings: a correlation for the influence of window to wall ratio and window orientation in Tripoli, Libya. J Build Eng 11:82–86. https://doi.org/10.1016/j.jobe.2017.04.003

ANSI/AWC (2014) Special Design Provisions for Wind and Seismic (SDPWS). American Wood Council

Anna Chatzopoulou M, Fisk D, Chatzopoulou M-A, Keirstead J, Markides N (2016) Characterising the Impact of HVAC design variables on buildings energy performance, using a global sensitivity analysis framework. https://www.researchgate.net/publication/311714388

Ascione F, Bianco N, Maria Mauro G, Napolitano DF (2019) Building envelope design: Multi-objective optimization to minimize energy consumption, global cost and thermal discomfort. Application to different Italian climatic zones. Energy 174:359–374. https://doi.org/10.1016/j.energy.2019.02.182

Bagheri MM, Doudak G (2020) Structural characteristics of light-frame wood shear walls with various construction detailing. Eng Struct 205. https://doi.org/10.1016/j.engstruct.2019.110093

Berwart S, Estrella X, Montaño J, Santa-María H, Almazán JL, Guindos P (2022) A simplified approach to assess the technical prefeasibility of multistory wood-frame buildings in high seismic zones. Eng Struct 257. https://doi.org/10.1016/j.engstruct.2022.114035

Casagrande D, Rossi S, Sartori T, Tomasi R (2012) Analytical and numerical analysis of timber framed shear walls. World Conf Timber Eng 2012:497–503. https://www.researchgate.net/publication/282605547

Cesari S, Valdiserri P, Coccagna M, Mazzacane S (2018) Energy savings in hospital patient rooms: the role of windows size and glazing properties. Energy Procedia 148:1151–1158. https://doi.org/10.1016/j.egypro.2018.08.027

Delgarm N, Sajadi B, Kowsary F, Delgarm S (2016) Multi-objective optimization of the building energy performance: a simulation-based approach by means of particle swarm optimization (PSO). Appl Energy 170:293–303. https://doi.org/10.1016/j.apenergy.2016.02.141

Dietz A, Vera S, Bustamante W, Flamant G (2020) Multi-objective optimization to balance thermal comfort and energy use in a mining camp located in the Andes Mountains at high altitude. Energy199. https://doi.org/10.1016/j.energy.2020.117121

Digehsara PA, Chegini SN, Bagheri A, Roknsaraei MP (2020) An improved particle swarm optimization based on the reinforcement of the population initialization phase by scrambled Halton sequence. Cogent Eng 7(1). https://doi.org/10.1080/23311916.2020.1737383

EN 1998-1 (2004) Eurocode 8: design of structures for earthquake resistance—part 1: general rules, seismic actions and rules for buildings. European Committee for Standardization (CEN), Brussels

Escobar RA, Cortés C, Pino A, Salgado M, Pereira EB, Martins FR, Boland J, Cardemil JM (2015) Estimating the potential for solar energy utilization in Chile by satellite-derived data and ground station measurements. Sol Energy 121:139–151. https://doi.org/10.1016/j.solener.2015.08.034

Estrella X, Malek S, Almazán JL, Guindos P, Santa María H (2021) Experimental study of the effects of continuous rod hold-down anchorages on the cyclic response of wood frame shear walls. Eng Struct 230. https://doi.org/10.1016/j.engstruct.2020.111641

Feng G, Chi D, Xu X, Dou B, Sun Y, Fu Y (2017) Study on the influence of window-wall ratio on the energy consumption of nearly zero energy buildings. Procedia Eng 205:730–737. https://doi.org/10.1016/j.proeng.2017.10.003

Goia F, Haase M, Perino M (2013) Optimizing the configuration of a façade module for office buildings by means of integrated thermal and lighting simulations in a total energy perspective. Appl Energy 108:515–527. https://doi.org/10.1016/j.apenergy.2013.02.063

Guindos P (2019) Fundamentos del diseño y la construcción con madera: vol I. (Fundamentals of timber design and construction: Vol. I). https://doi.org/10.4067/S0718-07642020000200001

Harkouss F, Fardoun F, Biwole PH (2018) Passive design optimization of low energy buildings in different climates. Energy 165:591–613. https://doi.org/10.1016/j.energy.2018.09.019

Hooke R, Jeeves TA (1961) "Direct Search" solution of numerical and statistical problems*. https://doi.org/10.1145/321062.321069

INN (1996) Diseño sísmico de edificios. (Seismic design of buildings). Instituto Nacional de Normalización INN-Chile. NCh433. Of96. (Chilean standard, in Spanish)

INN (2014) Madera - Construcciones en madera - Cálculo. (Timber - Timber constructions - Calculations). NCh 1198. Instituto Nacional de Normalización (Chilean standard, in Spanish)

ISO (2017) ISO6946 Building components and building elements - thermal resistance and thermal transmittance. International Organization for Standardization, Geneva, Switzerland

Jia J, Liu B, Ma L, Wang H, Li D, Wang Y (2021) Energy saving performance optimization and regional adaptability of prefabricated buildings with PCM in different climates. Case Stud Thermal Eng 26. https://doi.org/10.1016/j.csite.2021.101164

Klein SA (1976) TRNSYS-A transient simulation program. Ashrae Trans. 82:623

Lam TC, Ge H, Fazio P (2015) Impact of curtain wall configurations on building energy performance in the perimeter zone for a cold climate. Energy Procedia 78:352–357. https://doi.org/10.1016/j.egypro.2015.11.665

Lee JW, Jung HJ, Park JY, Lee JB, Yoon Y (2013) Optimization of building window system in Asian regions by analyzing solar heat gain and daylighting elements. Renewable Energy 50:522–531. https://doi.org/10.1016/j.renene.2012.07.029

Li H, Wang S, Cheung H (2018) Sensitivity analysis of design parameters and optimal design for zero/low energy buildings in subtropical regions. Appl Energy 228:1280–1291. https://doi.org/10.1016/j.apenergy.2018.07.023

Mahar WA, Verbeeck G, Reiter S, Attia S (2020) Sensitivity analysis of passive design strategies for residential buildings in cold semi-arid climates. Sustainability (Switzerland) 12(3). https://doi.org/10.3390/su12031091

Manfredi V, Masi A (2018) Seismic strengthening and energy efficiency: towards an integrated approach for the rehabilitation of existing RC buildings. Buildings 8(3). https://doi.org/10.3390/buildings8030036

Marino C, Nucara A, Pietrafesa M (2017) Does window-to-wall ratio have a significant effect on the energy consumption of buildings? A parametric analysis in Italian climate conditions. J Build Eng 13:169–183. https://doi.org/10.1016/j.jobe.2017.08.001

Mirrahimi S, Mohamed MF, Haw LC, Ibrahim NLN, Yusoff WFM, Aflaki A (2016) The effect of building envelope on the thermal comfort and energy saving for high-rise buildings in hot-humid climate. Renew Sustain Energy Rev 53:1508–1519. https://doi.org/10.1016/j.rser.2015.09.055. (Elsevier Ltd)

American Wood Council (2015) NDS National Design Specification for Wood Construction: With Commentary. American Wood Council

OGUC (2014) Ordenanza General de Urbanismo y Construcciones. (General Regulations for Urban Planning and Construction). Ministerio de la Vivienda y Urbanismo, Santiago, Chile. (Chilean standard, in Spanish)

Pohoryles DA, Maduta C, Bournas DA, Kouris LA (2020) Energy performance of existing residential buildings in Europe: a novel approach combining energy with seismic retrofitting. Energy Build 223. https://doi.org/10.1016/j.enbuild.2020.110024

Polastri A, Poh'siè GH, Paradisi I, Ratajczak J (2016) Energy and seismic performance of timber buildings in Mediterranean region. Structures and Architecture: Beyond their Limits. pp 161–168

Reilly A, Kinnane O (2017) The impact of thermal mass on building energy consumption. Appl Energy 198:108–121. https://doi.org/10.1016/j.apenergy.2017.04.024

Rojas F, Lew M, Naeim F (2010) An overview of building codes and standards in Chile at the time of the 27 February 2010 offshore Maule, Chile earthquake. Struct Des Tall Special Build 19(8):853–865. https://doi.org/10.1002/tal.676

Sarricolea P, Herrera-Ossandon M, Meseguer-Ruiz Ó (2017) Climatic regionalisation of continental Chile. J Maps 13(2):66–73. https://doi.org/10.1080/17445647.2016.1259592

Sayadi S, Hayati A, Salmanzadeh M (2021) Optimization of window-to-wall ratio for buildings located in different climates: An IDA-indoor climate and energy simulation study. Energies 14(7). https://doi.org/10.3390/en14071974

Thomas D, Ding G (2018) Comparing the performance of brick and timber in residential buildings – the case of Australia. Energy Build 159:136–147. https://doi.org/10.1016/j.enbuild.2017.10.094

Todd TZ, Briggs RS, Lucas RG (2003) Climate classification for building energy codes and standards: Part 2-zone definitions, maps, and comparisons. ASHRAE Trans 109:122

Tomasi R, Casagrande D, Grossi P, Sartori T (2015) Shaking table tests on a three-storey timber building. Proc Inst Civ Eng Struct Build 168(11):853–867. https://doi.org/10.1680/jstbu.14.00026

Ugalde D, Almazán JL, Santa María H, Guindos P (2019) Seismic protection technologies for timber structures: a review. Eur J Wood Prod 77(2):173–194. https://doi.org/10.1007/s00107-019-01389-9

Uribe D, Bustamante W, Vera S (2018) Potential of perforated exterior louvers to improve the comfort and energy performance of an office space in different climates. Build Simul 11(4):695–708. https://doi.org/10.1007/s12273-018-0435-y

Vera S, Pinto C, Tabares-Velasco PC, Bustamante W, Victorero F, Gironás J, Bonilla CA (2017a) Influence of vegetation, substrate, and thermal insulation of an extensive vegetated roof on the thermal performance of retail stores in semiarid and marine climates. Energy Build 146:312–321. https://doi.org/10.1016/j.enbuild.2017.04.037

Vera S, Uribe D, Bustamante W, Molina G (2017b) Optimization of a fixed exterior complex fenestration system considering visual comfort and energy performance criteria. Build Environ 113:163–174. https://doi.org/10.1016/j.buildenv.2016.07.027

Wenzel A, Vera S, Guindos P (2022) Integration of energy and seismic-structural design variables through the optimization of a multi-story residential light-frame timber building with different seismic lateral connectors and building stories. J Build Eng 57.https://doi.org/10.1016/j.jobe.2022.104831

Wetter M, Gov M (2016) GenOpt manual.http://SimulationResearch.lbl.gov

Xue P, Li Q, Xie J, Zhao M, Liu J (2019) Optimization of window-to-wall ratio with sunshades in China low latitude region considering

daylighting and energy saving requirements. Appl Energy 233–234:62–70. https://doi.org/10.1016/j.apenergy.2018.10.027

Yang Q, Liu M, Shu C, Mmereki D, Uzzal Hossain M, Zhan X (2015) Impact analysis of window-wall ratio on heating and cooling energy consumption of residential buildings in hot summer and cold winter zone in China. J Eng (United Kingdom)2015. https://doi.org/10.1155/2015/538254